The Structural Basis of Compstatin Activity Examined by Structure-Function-based Design of Peptide Analogs and NMR*⑤

Dimitrios Morikis‡§, Melinda Roy¶, Arvind Sahu‖, Anastasios Troganis‡‡, Patricia A. Jennings¶,
George C. Tsokos§§, and John D. Lambris¶¶‖**

*From the ‡Department of Chemical and Environmental Engineering, University of California, Riverside, California 92521,
the ¶Department of Chemistry and Biochemistry, University of California at San Diego, La Jolla, California 92093, the
‖National Centre for Cell Science, Pune University Campus, Ganeshkhind, Pune 411007, India, the ‡‡Department of
Biological Applications and Technologies, University of Ioannina, GR 45110 Ioannina, Greece, §§Walter Reed Army
Institute of Research, Silver Spring, Maryland 20910, and the ¶¶Department of Pathology and Laboratory Medicine,
University of Pennsylvania, Philadelphia, Pennsylvania 19104*

We have previously identified compstatin, a 13-residue cyclic peptide, that inhibits complement activation by binding to C3 and preventing C3 cleavage to C3a and C3b. The structure of compstatin consists of a disulfide bridge and a type I β-turn located at opposite sides to each other. The disulfide bridge is part of a hydrophobic cluster, and the β-turn is part of a polar surface. We present the design of compstatin analogs in which we have introduced a series of perturbations in key structural elements of their parent peptide, compstatin. We have examined the consistency of the structures of the designed analogs compared with compstatin using NMR, and we have used the resulting structural information to make structure-complement inhibitory activity correlations. We propose the following. 1) Even in the absence of the disulfide bridge, a linear analog has a propensity for structure formation consistent with a turn of a 3_{10}-helix or a β-turn. 2) The type I β-turn is a necessary but not a sufficient condition for activity. 3) Our substitutions outside the type I β-turn of compstatin have altered the turn population but not the turn structure. 4) Flexibility of the β-turn is essential for activity. 5) The type I β-turn introduces reversibility and sufficiently separates the two sides of the peptide, whereas the disulfide bridge prevents the termini from drifting apart, thus aiding in the formation of the hydrophobic cluster. 6) The hydrophobic cluster at the linked termini is involved in binding to C3 and activity but alone is not sufficient for activity. 7) β-Turn residues Gln^5 (Asn^5)-Asp^6-Trp^7(Phe^7)-Gly^8 are specific for the turn formation, but only Gln^5(Asn^5)-Asp^6-Trp^7-Gly^8 residues are specific for activity. 8) Trp^7 is likely to be involved in direct interaction with C3, possibly through the formation of a hydrogen bond. Finally we propose a binding model for the C3-compstatin complex.

Compstatin, a 13-residue cyclic peptide, is a novel complement inhibitor with the potential to be developed into a therapeutic agent (1). Compstatin binds to C3, which is a central complement component, through which all three pathways of complement activation, the classical, alternative, and lectin, converge (2). Although complement is part of the innate immune system while acting as a bridge between the innate and adaptive immune systems, and its activation is an important line of defense against invading foreign pathogens (3–5), its inappropriate activation can result in host cell damage (6). This is the case in more than 25 pathological conditions, including a number of autoimmune diseases, burn injuries, ischemia reperfusion injuries, stroke, dialysis, and cardiopulmonary bypass (see Ref. 7 for a complete list and references). The following have been shown. (*a*) Compstatin inhibits complement activation *in vitro* in human serum (8). (*b*) Compstatin totally inhibits *in vivo* heparin/protamine-induced complement activation in primates without side effects, in a situation that is typical in cardiac surgery (9). (*c*) Compstatin inhibits complement activation without toxicity in whole blood, in models of extracorporeal circuits, which resemble those used in cardiopulmonary bypass, dialysis, and plasmapheresis (10). (*d*) Compstatin prolongs the lifetime of porcine-to-human *ex vivo* perfused kidney xenograft model with human blood (11). (*e*) Finally, compstatin does not appear to have significant cytotoxicity as it showed little or no inhibition of clotting (12).

Compstatin was first identified as a 27-residue peptide using combinatorial phage-displayed random peptide library and was subsequently truncated, without loss of activity, to a 13-residue peptide (8). An attempt to further truncate the 13-residue peptide yielded inactive fragments (13). The sequence of compstatin is Ile^1-Cys^2-Val^3-Val^4-Gln^5-Asp^6-Trp^7-Gly^8-His^9-His^{10}-Arg^{11}-Cys^{12}-Thr^{13}-NH$_2$, where Cys^2 and Cys^{12} are disulfide-bonded. Reduction and alkylation of the two cysteines result in loss of inhibitory activity (8). We have determined previously the three-dimensional structure of compstatin in solution using NMR and a restrained hybrid distance geometry/simulated annealing methodology (14) and an alternative refinement methodology using global optimization (15). Compstatin forms

⑤ The on-line version of this article (available at *http://www.jbc.org*) contains the H^N(δ_1)-H^N(δ_2) backbone region of the DQF-COSY spectrum of the C2A/C12A analog and the H$^\alpha$/side chain (δ_1)-H^N(δ_2) region of the TOCSY spectra of Ac-H9A, Ac-V4A/H9A/T13I, Ac-V3A, Ac-W7F, Ac-Q5G/D6A/W7A, and Ac-Q5G/D6P/W7A analogs.

§ To whom correspondence may be addressed: Dept. of Chemical and Environmental Engineering, University of California, Riverside, CA 92521. Tel.: 909-787-2696; Fax: 909-787-5696; E-mail: dmorikis@engr.ucr.edu.

** Wellcome Trust Overseas Senior Research Fellow in Biomedical Science at the National Center for Cell Science, Ganeshkhind, Pune, India.

‖ To whom correspondence may be addressed: Dept. of Pathology and Laboratory Medicine, University of Pennsylvania, Philadelphia, PA 19104. Tel.: 215-746-5765; Fax: 215-573-8738; E-mail: lambris@mail.med.upenn.edu.

a type I β-turn spanning residues Gln[5]-Asp[6]-Trp[7]-Gly[8]. Measurements of inhibitory activities of compstatin analogs designed using an alanine scan in the sequence between residues Cys[2] and Cys[12] have shown that Val[3] and the four residues of
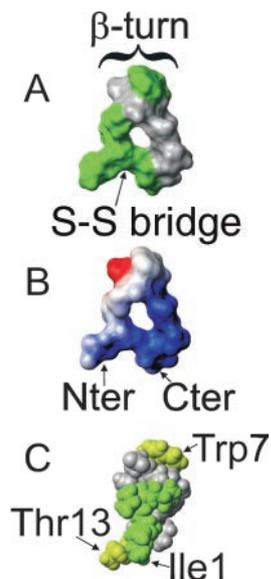

FIG. 1. *A*, the hydrophobic surface of compstatin. Hydrophobic residues are drawn in *green*, and the rest are drawn in *gray*. *B*, the electrostatic surface of compstatin, where *blue* and *red* correspond to residues with positive and negative charges, respectively. The orientation is the same as in *A*. *C*, a van der Waals sphere representation of compstatin that shows the continuity of the hydrophobic patch in a different view than in *A* and *B*. Residues Trp[7] and Thr[13] are colored in *light green* to denote less hydrophobicity, compared with Ile[1], Val[3], Val[4], Cys[2], Cys[12] (*darker green*). Note that this structure corresponds to non-acetylated compstatin at the amino terminus. The lowest energy structure of compstatin has been used from the ensemble of NMR structures deposited in the Protein Data Bank under code 1A1P (14). The program MOLMOL (29) has been used for molecular representation. *Nter*, amino terminus; *Cter*, carboxyl terminus.

the β-turn are essential for retaining activity (14). Alanine replacement for each one of the remaining residues resulted in reduced but not lost inhibitory activity (14). Fig. 1, *A* and *C*, shows the hydrophobic character of the structure of compstatin. We observe a hydrophobic clustering forming a patch at the linked termini involving residues Ile[1], Cys[2], Val[3], Val[4], Cys[12], Thr[13], whereas the ring of Trp[7] caps the β-turn with orientation toward the hydrophobic clustering. We have hypothesized that this hydrophobic clustering may be essential for structural stability and inhibitory activity of compstatin (1, 14). Fig. 1*B* shows the electrostatic character of compstatin. Positive charges from His[9], His[10] (each about 50% protonated at the experimental pH), and Arg[11] and a negative charge from Asp[6] are observed at the opposite side of the hydrophobic cluster. However, a positive charge from the amino terminus is disrupting the hydrophobic cluster. This charge was neutralized by acetylation of the amino terminus in our effort to avoid cleavage of the peptide bond between Ile[1] and Cys[2] during the biotransformation of compstatin (13). Interestingly, upon acetylation activity of compstatin was increased by a factor of 3 (13). We then designed our subsequent studies using the more effective sequence of Ac-Ile[1]-Cys[2]-Val[3]-Val[4]-Gln[5]-Asp[6]-Trp[7]-Gly[8]-His[9]-His[10]-Arg[11]-Cys[12]-Thr[13]-NH$_2$.

Because of its activity, low toxicity, and structural simplicity compstatin is a promising candidate for drug development (1, 12, 13). It is not unusual for a short cyclic peptide to become an oral drug; a successful example is the widely used immunosuppressant cyclosporin (16). Also, it is known that several immunogenic peptides adopt functional β-turn structures (17, 18). In an earlier study we designed and tested a number deletion analogs of compstatin in an attempt to truncate further the 13-residue peptide, but none of them was active (13). Neither a retro-inverso analog nor β-turn analogs, with substitutions that we expected to enhance a type I or a type II β-turn, were active (13).

With the goal to improve on the activity of compstatin, we have initiated the rational design of compstatin analogs based

TABLE I

Inhibitory activities of compstatin analogs studied by NMR and their parent peptides[a]

Peptide[b]	Sequence[c]	IC$_{50}$ (μM)[d]	Activity
Compstatin	I*CVVQDWGHHRC*T-NH$_2$	12	Active
Compstatin ring-only	*CVVQDWGHHRC*	33[e]	Active
Ac-Compstatin	Ac-I*CVVQDWGHHRC*T-NH$_2$	4.5[f]	Active
C2A/C12A	I AVVQDWGHHRA T-NH$_2$	>500	Inactive
Ac-H9A	Ac-I*CVVQDWGAHRC*T-NH$_2$	2.9	Active
Ac-V4A/H9A/T13I	Ac-I*CVAQDWGAHRC*I-NH$_2$	4	Active
Ac-V3A	Ac-I*CAVQDWGHHRC*T-NH$_2$	NA[g]	NA
V3A ring-only	*CAVQDWGHHRC* -NH$_2$	>1200[e]	Inactive
Ac-W7F	Ac-I*CVVQDFGHHRC*T-NH$_2$	>400	Inactive
Ac-Q5G/D6A/W7A	Ac-I*CVVGAAGHHRC*T-NH$_2$	>100	Inactive
Ac-Q5G/D6P/W7F	Ac-I*CVVGPFGHHRC*T-NH$_2$	>400[f]	Inactive

[a] Underlined residues are points of amino acid replacement or acetyl group addition.
[b] Ac stands for acetylated N terminus.
[c] Asterisks on the left and right of Cys[2] and Cys[12], respectively, denote disulfide-linked cysteines.
[d] Complement activities were determined by measuring alternative pathway-mediated erythrocyte lysis.
[e] From Morikis *et al.* (14).
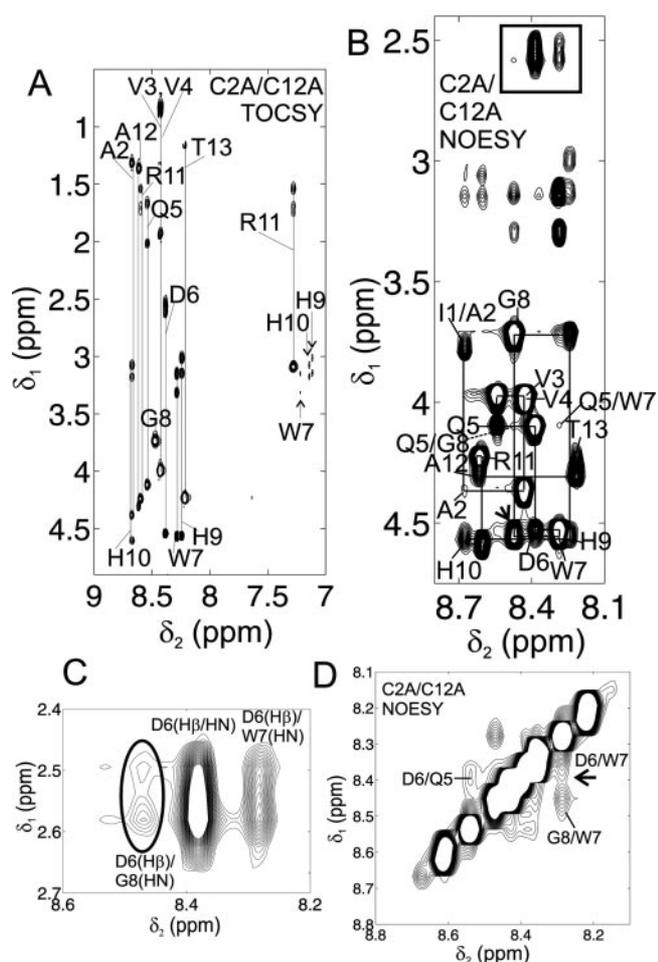[f] From Sahu *et al.* (13).
[g] Not available.

NMR Studies of Compstatin Analogs

FIG. 2. **NMR spectra of the C2A/C12A compstatin analog.** *A*, portion of the side chain/H$^\alpha$(δ_1)-H^N(δ_2) region of the TOCSY spectrum. Resonances with chemical shifts below 7.5 ppm belong to side chains and above 7.5 ppm belong to backbone. *Straight lines* connect cross-peaks corresponding to the same residue and are labeled appropriately. *B*, the H$^\alpha$/H$^\beta$(δ_1)-H^N(δ_2) region of the NOESY spectrum. Sequential NOE connectivities corresponding to intra-residue H$^\alpha$(i)-H^N(i) and short range inter-residue H$^\alpha$(i)-H^N($i + 1$) are shown, but only intra-residue NOEs are labeled for simplicity. Because of spectral overlap (*arrow*), it is not possible to identify the presence or absence of an Asp^6 H$^\alpha$-Gly^8 H^N NOE, which is characteristic of a β-turn. An Asp^6 H$^\beta$-Gly^8 H^N NOE is observed in the boxed region of the spectrum. The *dotted line* shows an H$^\alpha$(i)-H^N($i + 3$) NOE (see text). *C*, the *boxed region* of *B* was plotted at lower contour level threshold with the Asp^6 H$^\beta$-Gly^8 H^N NOE *circled*. *D*, the H^N(δ_1)-H^N(δ_2) region of the NOESY spectrum. Symmetry related cross-peaks are labeled once at either side of the diagonal.

on the available solution structure and function data. We have constructed 7 analogs by introducing perturbations in the key components of the structure of compstatin, which we have studied using homonuclear two-dimensional NMR spectra. Our goal is to classify which residues are essential for structural stability, activity, or both. Also, we aim to elucidate the roles of the disulfide bridge, of the hydrophobic patch, and of the charges of compstatin in both structural stability and binding/inhibitory activity. Certain substitutions have resulted in retaining or slightly increasing the inhibitory activity while maintaining the structural stability. Other substitutions have resulted in loss of inhibitory activity while maintaining the characteristic β-turn found in compstatin. Finally, some substitutions have resulted in loss of both structural stability and activity. We present here the design of the 7 analogs, one of which is slightly more active than compstatin and one that is equally as active as compstatin.

Despite the presence of multiple conformations (due to flex-

ibility) of small peptides in solution, NMR has been widely used to determine the presence of conformers with distinguishable populations in linear and cyclic peptides, peptide fragments derived from protein sequences, immunogenic peptides, and peptides of *de novo* design (*e.g.* see Refs. 17–23, and references therein). These studies typically require the use of two-dimensional correlation spectroscopy (TOCSY,[1] DQF-COSY) for resonance assignments and residue identification and two-dimensional NOE/ROE spectroscopy (NOESY and ROESY) to establish NOE connectivity patterns that are consistent with specific structure (20). In certain cases, coupling constants, chemical shifts, and temperature coefficients of chemical shifts are also helpful.

Based on the structural data we present here and our earlier experimental work on structure, binding kinetics, and activity, we propose a model for recognition and binding of compstatin to C3.

MATERIALS AND METHODS

Peptide synthesis and purification was performed as described previously (8, 14). Inhibitory activity of compstatin and its analogs on the complement system was studied by measuring their effect on the alternative pathway. Complement activation inhibition was assessed by measuring the lysis of rabbit erythrocytes in normal human serum, as described previously (8, 14). All analogs were examined by mass spectroscopy and found to be monomeric. The analogs of compstatin used for NMR studies were acetylated with the exception of the C2A/C12A analog. The NMR samples were prepared in 90% H$_2$O, 10% D$_2$O buffer containing 50 mM potassium phosphate, 100 mM potassium chloride, 0.1% sodium azide, and 10 μM EDTA. Sample pH was ~6 for the C2A/C12A, Ac-V3A, Ac-W7F, Ac-Q5G/D6A/W7A, and Ac-Q5G/D6P/W7F analogs and 6.5 for the Ac-H9A and Ac-V4A/H9A/T13I analogs. Peptide concentrations were in the range of 1.5–5 mM, depending on the analog. NMR spectra were recorded at 5 °C.

NMR spectra for the Ac-V3A, Ac-W7F, Ac-H9A, C2A/C12A, Ac-V4A/H9A/T13I, and Ac-Q5G/D6A/W7A analogs were collected using Bruker DMX 500 MHz spectrometer and for the Ac-Q5G/D6P/W7F were collected using a Bruker AMX 400 MHz spectrometer. DQF-COSY, TOCSY, and NOESY spectra were collected for all analogs using standard pulse sequences (see Ref. 24 and references therein). All spectra were collected using the 3-9-19 pulse sequence with gradients for water suppression (25). The NOE mixing time was 500 ms and the TOCSY mixing time was 60 ms for the Ac-V3A, Ac-W7F, Ac-H9A, C2A/C12A, Ac-V4A/H9A/T13I, and Ac-Q5G/D6A/W7A analogs. The NOE mixing time was 400 ms, and the TOCSY mixing time was 75 ms for the Ac-Q5G/D6P/W7F analog.

Spectral processing was performed using matNMR, which is a toolbox for processing NMR/EPR data (www.nmr.ethz.ch/matnmr; written by Jacco van Beek) under MATLAB (The Mathworks, Inc., Natick, MA) and for the Ac-Q5G/D6P/W7F analog using Felix (Molecular Simulations Inc., San Diego, CA). In t_2 dimension apodization was performed using Gaussian window functions for the DQF-COSY and NOESY spectra and cosine squared window functions for the TOCSY spectra. In t_1 dimension cosine squared window functions were used for all spectra. The solvent was deconvoluted from the spectra using the time domain convolution method of Marion *et al.* (26) with a sine bell function.

RESULTS

Table I shows the analogs of compstatin we have studied by NMR and their inhibitory activities. These are the single replacement analogs Val^3 → Ala (Ac-V3A), Trp^7 → Phe (Ac-W7F), and His^9 → Ala (Ac-H9A), the double replacement analog Cys^2 → Ala/Cys^{12} → Ala (C2A/C12A), and the triple replacement analogs Val^4 → Ala/His^9 → Ala/Thr^{13} → Ile (Ac-V4A/H9A/T13I), Gln^5 → Gly/Asp^6 → Ala/Trp^7 → Ala (Ac-Q5G/D6A/W7A), and Gln^5 → Gly/Asp^6 → Pro/Trp^7 → Phe (Ac-Q5G/D6P/W7F). Given that we know the solution structure of compstatin (14) we can now examine by using NMR the following: 1) if the

---

[1] The abbreviations used are: TOCSY, total correlation spectroscopy; DQF-COSY, double quantum filtered correlated spectroscopy; NOE, nuclear Overhauser effect; NOESY, NOE spectroscopy.
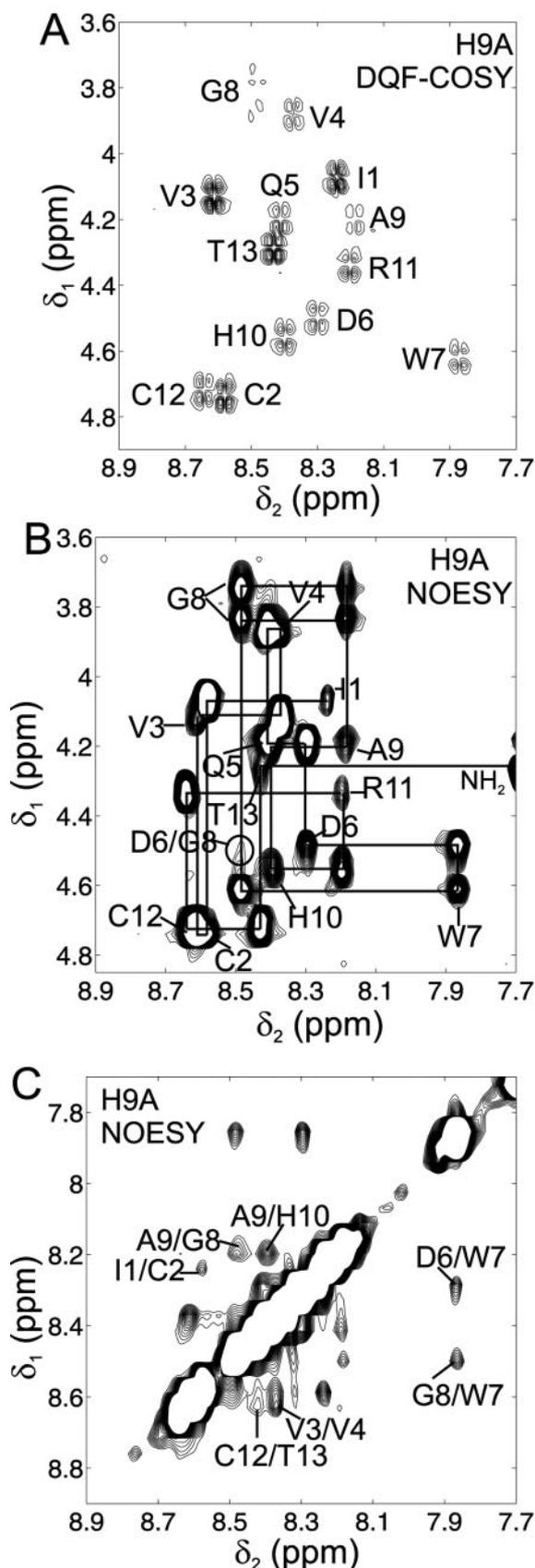
FIG. 3. **NMR spectra of the Ac-H9A compstatin analog.** *A*, portion of the Hα(δ₁)-Hᴺ(δ₂) region of the DQF-COSY spectrum showing the backbone of the peptide. *B*, the Hα(δ₁)-Hᴺ(δ₂) region of the NOESY spectrum. Sequential NOE connectivities corresponding to intra-residue Hα(*i*)-Hᴺ(*i*) and short range inter-residue Hα(*i*)-Hᴺ(*i* + 1) are shown, but only the intra-residue NOEs are labeled for simplicity. A weak cross-peak (*circled*) corresponds to the Asp⁶ Hα-Gly⁸ Hᴺ NOE,

designed analogs form structures consistent with the type I β-turn of compstatin or with some other type of turn or secondary structure; 2) the role of the disulfide bridge in the formation of structure in compstatin; 3) the role of the hydrophobic and polar surfaces in the structural stability of compstatin; and 4) which of the above structural characteristics are essential for function.

We begin our analysis by focusing on the two major types of β-turns, type I and II. We test the consistency of the observed NOEs with the expected NOEs for type I and type II β-turns. This can be accomplished by examining the following NOEs: Hᴺ(2)-Hᴺ(3), Hᴺ(3)-Hᴺ(4), Hα(2)-Hᴺ(3), Hα(3)-Hᴺ(4), and Hα(2)-Hᴺ(4), where the numbers in parentheses refer to residues 2, 3, and 4 of the β-turn (20). NOEs Hα(2)-Hᴺ(3) and Hα(3)-Hᴺ(4) should always be present in the case of a β-turn, but they are also generic NOEs in the case of extended structure. The weak NOE Hα(2)-Hᴺ(4) is characteristic of the presence of a β-turn of both types, type I and type II. A strong Hᴺ(3)-Hᴺ(4) NOE is also characteristic of the presence of a β-turn of both types, type I and type II. The NOE that distinguishes a type I from a type II β-turn is the Hᴺ(2)-Hᴺ(3), which has strong intensity in the case of a type I β-turn and weak intensity in the type II β-turn. The turn assignment can be further refined by looking at the intensities of the Hα(2)-Hᴺ(3) NOE, which should be medium for a type I β-turn and strong for type II β-turn (20).

The Linear Analog with Cys² →Ala/Cys¹² →Ala (C2A/C12A) Double Replacement—In the C2A/C12A analog the two cysteines are replaced by alanines, making it a linear peptide. This is an inactive peptide (Table I). The rationale for the design of the linear C2A/C12A analog was to test the significance of the disulfide bridge in restricting the conformational space of compstatin and in the formation of the type I β-turn.

Fig. 2*A* shows the Hα/side chain(δ₁)-Hᴺ(δ₂) region of the TOCSY spectrum of the C2A/C12A analog, where all residues with the exception of Ile1 have been identified. (Note that this analog is not acetylated which makes the amide of the of the first residue unobservable because of fast exchange with the solvent.) Chemical shift overlaps in both the Hα and Hᴺ of Val³/Val⁴, and to a lesser extent Arg¹¹/Ala¹² are present. Also, chemical shift overlaps in the Hα of Trp⁷/His⁹, and to a lesser extent Asp⁶/Trp⁷/His⁹ are present. Finally, chemical shift overlaps in the Hᴺ of Ala²/His¹⁰ are present. These overlaps are characteristic of the flexibility of this analog.

Fig. 2*B* shows the Hα/Hβ(δ₁)-Hᴺ(δ₂) region of the NOESY spectrum of the C2A/C12A analog. Sequential connectivities corresponding to intra-residue Hα(*i*)-Hᴺ(*i*) and short range Hα(*i*)-Hᴺ(*i* + 1) NOE cross-peaks are marked in Fig. 2*B*, but only the intra-residue cross-peaks are labeled for simplicity. Unfortunately, because of the overlap of the Hαs of Asp⁶/Trp⁷, we cannot distinguish the presence of a weak Hα(*i*)-Hᴺ(*i* + 2) cross-peak for the Asp⁶ Hα-Gly8 Hᴺ NOE from the strong Trp⁷ Hα-Gly⁸ Hᴺ cross-peak (Fig. 2*B*, *arrow*), which would be consistent with β-turn of the parent peptide, compstatin. This led us to look closer at the Hβ(δ₁)/Hᴺ(δ₂) region of the spectrum where indeed a very weak Hβ(*i*)-Hᴺ(*i* + 2) cross-peak is present corresponding to the Asp⁶ Hβ-Gly⁸ Hᴺ NOE (Fig. 2, *B* and *C*). This cross-peak is consistent with the presence of a turn population in the segment Gln⁵-Asp⁶-Trp⁷-Gly⁸ as in parent pep-

which is characteristic of the presence of a β-turn in the same region as in the parent peptide compstatin. *C*, the Hᴺ(δ₁)-Hᴺ(δ₂) region of the NOESY spectrum. Cross-peaks corresponding to Asp⁶ Hᴺ-Trp⁷ Hᴺ and Trp⁷ Hᴺ-Gly⁸ Hᴺ NOEs are observed, which are characteristic of the presence of a type I β-turn in the same region as in the parent peptide compstatin. Symmetry related cross-peaks are labeled once at either side of the diagonal.
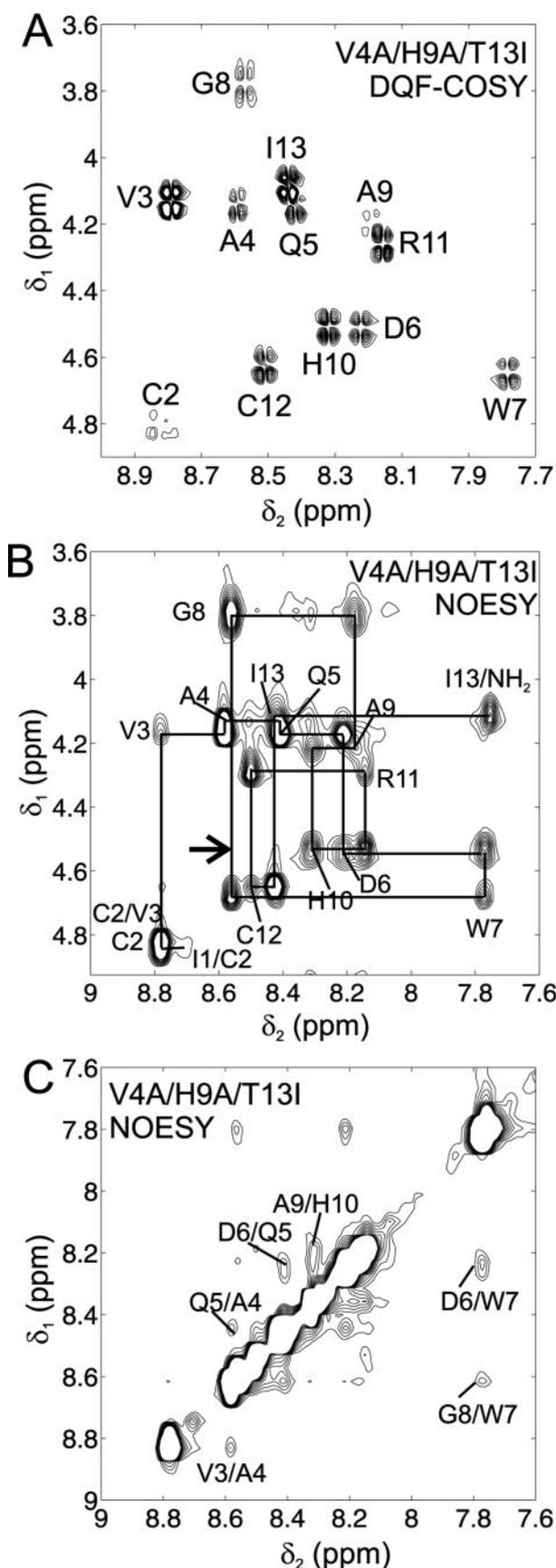
NMR Studies of Compstatin Analogs

FIG. 4. **NMR spectra of the Ac-V4A/H9A/T13I compstatin analog.** Cross-peak labeling is as in Fig. 3. *A*, portion of the $H^\alpha(\delta_1)$-$H^N(\delta_2)$ region of the DQF-COSY spectrum showing the backbone of the peptide. *B*, the $H^\alpha(\delta_1)$-$H^N(\delta_2)$ region of the NOESY spectrum. The *arrow* shows the absence of a weak cross-peak corresponding to the Asp[6]

tide compstatin. Further examination of $H^N(\delta_1)$-$H^N(\delta_2)$ region of the NOESY spectrum (Fig. 2*D*) reveals a medium Trp[7] H^N-Gly[8] H^N cross-peak. An Asp[6] H^N-Trp[7] H^N cross-peak is also present but somehow obscured by the diagonal (Fig. 2*D*). These two cross-peaks are consistent with the presence of a type I β-turn in the segment Gln[5]-Asp[6]-Trp[7]-Gly[8], as in parent peptide compstatin. Closer examination of the spectra in Fig. 2, *B* and *D*, reveals the presence of Gln[5] H^α-Trp[7] H^N and Gln[5] H^N-Asp[6] H^N cross-peaks, which in combination with the Asp[6] H^N-Trp[7] H^N cross-peak are characteristic of the presence of a type I β-turn in the segment Val[4]-Gln[5]-Asp[6]-Trp[7]. Alternatively, we can say that two fused type I β-turns are present in the segment Val[4]-Gln[5]-Asp[6]-Trp[7]-Gly[8]. A weak $H^\alpha(i)$-$H^N(i + 3)$ cross-peak, Gln[5] H^α-Gly[8] H^N (Fig. 2*B*), in combination with the $H^\alpha(i)$-$H^N(i + 2)$ and $H^N(i)$-$H^N(i + 1)$ cross-peaks mentioned above for the fused β-turns, is suggestive of the presence of a population forming a turn of a 3_{10}-helix (20) in the segment Gln[5]-Asp[6]-Trp[7]-Gly[8].

Based on the observed NOEs for the C2A/C12A analog and the β-turn forming analogs (see below), we conclude that the linear sequence of compstatin has a propensity to form a 3_{10}-helix, which upon formation of the disulfide bond is reduced to a β-turn. Interestingly, a type III β-turn is classified as a turn of a 3_{10}-helix (19, 27). A type III β-turn has characteristic dihedral angles for residues 2 and 3 of the turn $(\phi_2, \psi_2) = (-60°, -30°)$ and $(\phi_3, \psi_3) = (-60°, -30°)$ compared with a type I β-turn which has dihedral angles $(\phi_2, \psi_2) = (-60°, -30°)$ and $(\phi_3, \psi_3) = (-90°, 0°)$. However, because there is a statistical variation associated with dihedral angles of $\pm 30°$ (which is also the error of calculated dihedral angles from NMR data), the type III β-turn is often classified under the type I β-turn category. In this report we do not distinguish a type III from a type I β-turn. The structure of the C2A/C12A analog is not sufficient for C3 binding and activity (Table I), which makes the disulfide bridge necessary for activity. Based on the structure of compstatin (Fig. 1), we propose that the disulfide bridge brings together the termini of compstatin thus contributing to the formation of the hydrophobic patch, which in turn is necessary for recognition and binding to C3.

The Single Replacement His[9] → Ala (Ac-H9A) Analog—In the Ac-H9A analog the His[9], right outside the C-terminal residue of the β-turn, is replaced by Ala. This is an analog slightly more active than its parent peptide, Ac-compstatin (Table I). The rationale for the design of the Ac-H9A analog was to introduce additional conformational freedom at one end of the type I β-turn by removing the bulky histidine and replacing it with the smaller alanine. This accomplishes a test for the turn stability without losing activity, given that a non-acetylated ring-only form of this analog (with missing residues Ile[1] and Thr[13] outside the peptide ring) was active, although less active than its parent peptide ring-only compstatin (Table I of Ref. 14).

Fig. 3*A* shows the $H^\alpha(\delta_1)$-$H^N(\delta_2)$ region of the DQF-COSY spectrum of the Ac-H9A analog, where all residues have been identified. Chemical shift overlaps in the H^α are observed for Cys[2]/Cys[12] and Gln[5]/Ala[9]. Chemical shift overlaps in the H^N are observed for of Ala[9]/Arg[11] and Gln[5]/Thr[13].

Fig. 3*B* shows the $H^\alpha(\delta_1)$-$H^N(\delta_2)$ region of the NOESY spectrum of the Ac-H9A analog. Sequential connectivities corresponding to intra-residue $H^\alpha(i)$-$H^N(i)$ and short range $H^\alpha(i)$-

H^α-Gly[8] H^N NOE, which would be characteristic of the presence of a β-turn in the same region as in the parent peptide compstatin. *C*, the $H^N(\delta_1)$-$H^N(\delta_2)$ region of the NOESY spectrum. Asp[6] H^N-Trp[7] H^N and Trp[7] H^N-Gly[8] H^N NOEs are observed, which are characteristic of the presence of a type I β-turn in the same region as in the parent peptide compstatin.

$H^N(i + 1)$ NOE cross-peaks are marked in the figure. In addition, a weak $H^\alpha(i)$-$H^N(i + 2)$ cross-peak corresponding to Asp[6] H^α-Gly[8] H^N is observed (*circled* in Fig. 3*B*), which is consistent with the presence of a β-turn. Fig. 3*C* shows the $H^N(\delta_1)$-$H^N(\delta_2)$ region of the NOESY spectrum of the Ac-H9A analog where observed $H^N(i)$-$H^N(i + 1)$ cross-peaks are labeled. Medium intensity cross-peaks corresponding to Asp[6] H^N-Trp[7] H^N and Trp[7] H^N-Gly[8] H^N NOEs are observed which are consistent with the presence of a type I β-turn in the segment Gln[5]-Asp[6]-Trp[7]-Gly[8], as in compstatin. In compstatin, a very weak $H^\beta(i)$-$H^N(i + 2)$ NOE of Asp[6] H^β-Gly[8] H^N was also observed (14), which is absent in the Ac-H9A analog (data not shown). This suggests a slightly increased flexibility or alternatively slightly reduced population of the type I β-turn in Ac-H9A analog compared with compstatin.

The above NOE data are consistent with the presence of a weak (with small but observable population) type I β-turn in the segment Gln[5]-Asp[6]-Trp[7]-Gly[8] of Ac-H9A analog, as was the case of parent peptide compstatin. In compstatin, the presence of Gly[8] at position 4 of the type I β-turn was deemed necessary to reduce side chain steric hindrance for turn reversal. By replacing the next residue His[9] by Ala, we introduced additional flexibility outside one end of the β-turn by increasing the available conformational space. This additional flexibility did not alter the type I β-turn structure, although it slightly reduced its population. It is worth noting that the population of the type β-turn in compstatin was estimated at 42–63% (14), which suggests flexibility in the parent peptide as well. This analog possesses slightly higher inhibitory activity than compstatin (Table I), which suggests that flexibility outside the β-turn contributes to activity.

The Triple Replacement Val[4] → Ala/His[9] → Ala/Thr[13] → Ile (Ac-V4A/H9A/T13I) Analog—In the Ac-V4A/H9A/T13I analog not only His[9] but also Val[4], right outside both ends of the β-turn, are replaced by alanines, with the rationale of introducing even more conformational freedom outside the turn, than in the Ac-H9A analog. In addition, Thr[13] is replaced with the more hydrophobic isoleucine to enhance the hydrophobic clustering at the termini. This analog is equally active as compstatin (Table I).

Fig. 4*A* shows the $H^\alpha(\delta_1)$-$H^N(\delta_2)$ region of the DQF-COSY spectrum of the Ac-V4A/H9A/T13I analog, where all residues except Ile[1] have been identified (Ile[1] has been identified in the TOCSY spectrum, see the Supplemental Material). Chemical shift overlap in the H^α is observed for Asp[6]/His[10]. Chemical shift overlaps in the H^N are observed for Ala[4]/Gly[8], Gln[5]/Ile[13], and Ala[9]/Arg[11]. Despite the overlaps in individual dimensions, the resulting cross-peaks are distinct (Fig. 4*A*).

Fig. 4*B* shows the $H^\alpha(\delta_1)$-$H^N(\delta_2)$ region of the NOESY spectrum of the Ac-V4A/H9A/T13I analog. All sequential connectivities corresponding to intra-residue $H^\alpha(i)$-$H^N(i)$ and short range $H^\alpha(i)$-$H^N(i + 1)$ NOE cross-peaks are observed and marked in the figure. However, a weak $H^\alpha(i)$-$H^N(i + 2)$ cross-peak for the Asp[6] H^α-Gly[8] H^N NOE is not observed (position indicated by an *arrow* in Fig. 4*B*). Fig. 4*C* shows the $H^N(\delta_1)$-$H^N(\delta_2)$ region of the NOESY spectrum of the Ac-V4A/H9A/T13I analog, where observed $H^N(i)$-$H^N(i + 1)$ NOEs are labeled. Medium/weak intensity cross-peaks corresponding to Asp[6] H^N-Trp[7] H^N and Trp[7] H^N-Gly[8] H^N NOEs are observed, which are consistent with the presence of a type I β-turn in the segment Gln[5]-Asp[6]-Trp[7]-Gly[8], as in compstatin. It should be noted that the absence of the Asp[6] H^α-Gly[8] H^N NOE suggests a reduced turn population in the Ac-V4A/H9A/T13I analog compared with the Ac-H9A analog.

The above NOE data are consistent with the presence of a small population of type I β-turn in the Gln[5]-Asp[6]-Trp[7]-Gly[8]

segment of the Ac-V4A/H9A/T13I analog, which is smaller than the turn population in the same segment of the Ac-H9A analog. Despite the increase of conformational freedom and weakening of the type I β-turn, this peptide is an analog equally active to compstatin (Table I).

The fact that both Ac-H9A and Ac-V4A/H9A/T13I but not the linear C2A/C12A analog are active suggests that flexibility between the β-turn and disulfide bridge structures is necessary for binding activity.

The Single Replacement Val[3] → Ala (Ac-V3A) Analog—In the Ac-V3A analog Val[3] is replaced by Ala. The rationale for this replacement was to weaken the hydrophobic clustering at the termini. This replacement resulted in an inactive analog (Table I).

Fig. 5*A* shows the $H^\alpha(\delta_1)$-$H^N(\delta_2)$ region of the DQF-COSY spectrum of the Ac-V3A analog, where all residues have been identified. Chemical shift overlaps in both H^α and H^N are observed for Asp[6]/His[9]. Chemical shift overlaps in the H^α are observed for Cys[2]/Cys[12] and to a lesser extent for Ala[3]/Arg[11]. Chemical shift overlaps in the H^N are observed for Asp[6]/Trp[7]/His[9] and Gln[5]/Arg[11]. Interestingly, the Ac-V3A replacement had an impact in the chemical shift of Asp[6], which is shifted upfield (Fig. 5*A*) compared with the other analogs (Figs. 2*A*, 3*A*, and 4*A*).

Fig. 5*B* shows the $H^\alpha(\delta_1)$-$H^N(\delta_2)$ region of the NOESY spectrum of the Ac-V3A analog. All sequential connectivities corresponding to intra-residue $H^\alpha(i)$-$H^N(i)$ and short range $H^\alpha(i)$-$H^N(i + 1)$ NOE cross-peaks are observed and marked in the figure. In addition, a medium $H^\alpha(i)$-$H^N(i + 2)$ cross-peak is observed corresponding to NOE Asp[6] H^α-Gly8 H^N, which is characteristic of the presence of a β-turn in the segment Gln[5]-Asp[6]-Trp[7]-Gly[8]. Fig. 5*C* shows the $H^N(\delta_1)$-$H^N(\delta_2)$ region of the NOESY spectrum of the Ac-V3A analog, where observed $H^N(i)$-$H^N(i + 1)$ NOEs are labeled. Two strong cross-peaks corresponding to NOEs between Gln[5] H^N-Asp[6] H^N and Trp[7] H^N-Gly[8] H^N are observed, but because of the overlap of the amide protons of Asp[6] and Trp[7] we cannot determine or exclude the presence of the Asp[6] H^N-Trp[7] H^N cross-peak. Because of the intensities of the observed NOEs, we deduce that the observed structure is consistent with the presence of a strong type I β-turn in the segment Gln[5]-Asp[6]-Trp[7]-Gly[8], as in parent peptide compstatin.

Based on the NOE data of the Ac-V3A analog, the Val[3] → Ala replacement has resulted in a stronger (of higher population) type I β-turn. It appears that the remote, in relation with the β-turn of compstatin, residue Val[3] somehow influences the β-turn stability in the parent peptide. Because the activity of the Ac-V3A analog is lost (Table I), we can say that Val[3] influences the binding of the parent peptide compstatin to C3, possibly either through the hydrophobic clustering of the termini or through some type of stabilization of the β-turn. The simultaneous presence of both effects cannot be excluded.

The Single Replacement Trp[7] → Phe (Ac-W7F) Analog—In the Ac-W7F analog Trp[7] is replaced by Phe. The rationale for this replacement was to enhance the hydrophobicity of the β-turn and participation of residue 7 in the hydrophobic clustering, if any (Fig. 1*A*). This replacement resulted in an inactive analog (Table I).

Fig. 6*A* shows the $H^\alpha(\delta_1)$-$H^N(\delta_2)$ region of the DQF-COSY spectrum of the Ac-W7F analog, where all residues have been identified. Chemical shift overlaps in the H^α are observed for Cys[2]/Cys[12] and Gln[5]/Thr[13]. Chemical shift overlaps in the H^N are observed for Phe[7]/His[9], Gln[5]/Arg[11], and His[10]/Cys[12]. Despite the overlaps in individual dimensions, the resulting cross-peaks are distinct (Fig. 6*A*).

Fig. 6, *B* and *C*, shows the $H^\alpha(\delta_1)$-$H^N(\delta_2)$ and $H^N(\delta_1)$-$H^N(\delta_2)$
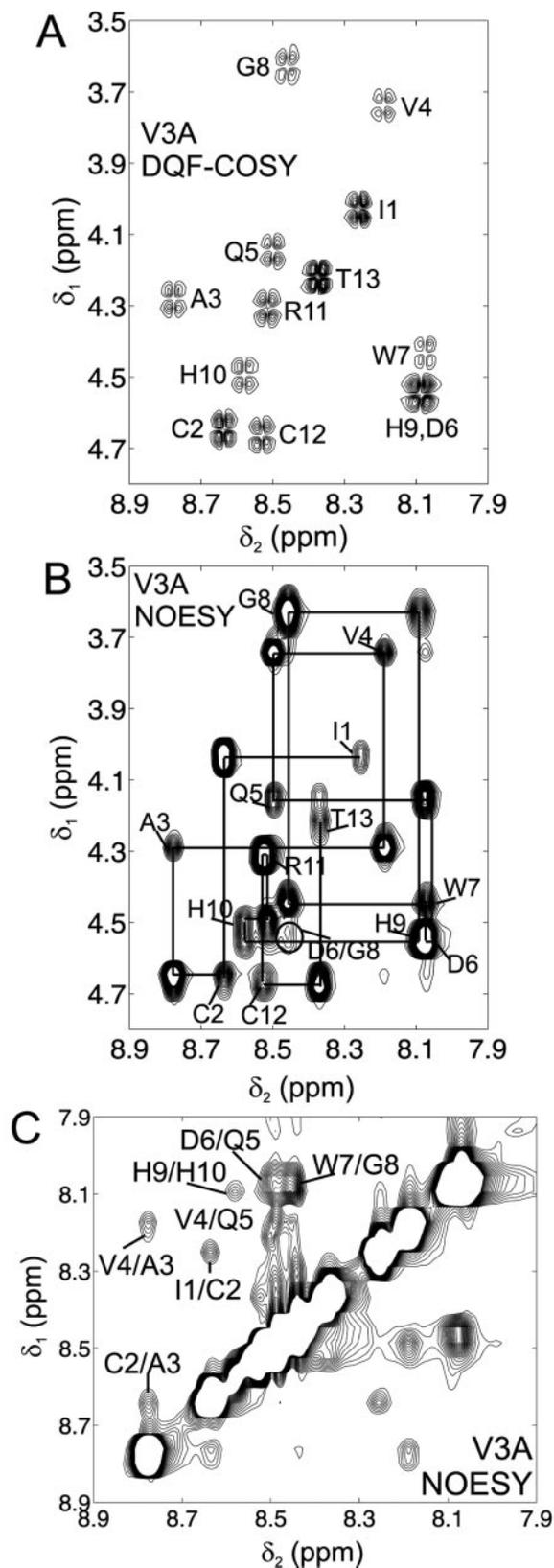
NMR Studies of Compstatin Analogs

FIG. 5. **NMR spectra of the Ac-V3A compstatin analog.** Cross-peak labeling is as in Fig. 3. *A*, portion of the $H^\alpha(\delta_1)$-$H^N(\delta_2)$ region of the DQF-COSY spectrum showing the backbone of the peptide. *B*, the $H^\alpha(\delta_1)$-$H^N(\delta_2)$ region of the NOESY spectrum. A medium intensity cross-peak (*circled*) corresponds to the Asp^6 H^α-Gly^8 H^N NOE, which is consistent with the presence of β-turn in the same region as in the parent peptide compstatin. *C*, the $H^N(\delta_1)$-$H^N(\delta_2)$ region of the NOESY spectrum. Cross-peaks corresponding to Gln^5 H^N-Asp^6 H^N and Trp^7 H^N-Gly^8 H^N NOEs are observed, but the overlap of the amide protons of Asp^6 and Trp^7 does not allow us to cleanly identify a Asp^6 H^N-Trp^7 H^N NOE.
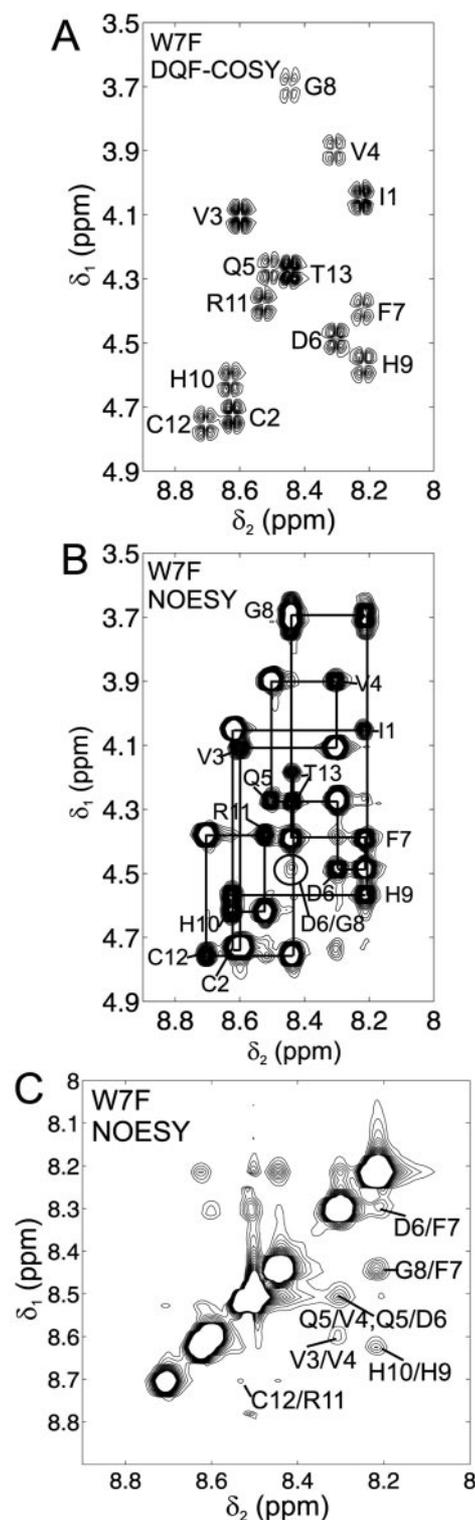

FIG. 6. **NMR spectra of the Ac-W7F compstatin analog.** Cross-peak labeling is as in Fig. 3. *A*, portion of the $H^\alpha(\delta_1)$-$H^N(\delta_2)$ region of the DQF-COSY spectrum showing the backbone of the peptide. *B*, the $H^\alpha(\delta_1)$-$H^N(\delta_2)$ region of the NOESY spectrum. The *circled* cross-peak corresponds to the Asp^6 H^α-Gly^8 H^N NOE, which is consistent with the presence of β-turn in the same region as in the parent peptide compstatin. *C*, the $H^N(\delta_1)$-$H^N(\delta_2)$ region of the NOESY spectrum. Cross-peaks corresponding to Asp^6 H^N-Trp^7 H^N and Trp^7 H^N-Gly^8 H^N NOEs are observed, which are characteristic of the presence of a type I β-turn in the same region as the parent peptide compstatin.

regions, respectively, of the NOESY spectrum of the Ac-W7F analog. All sequential connectivities corresponding to intra-residue $H^\alpha(i)$-$H^N(i)$ and short range $H^\alpha(i)$-$H^N(i + 1)$ NOE cross-
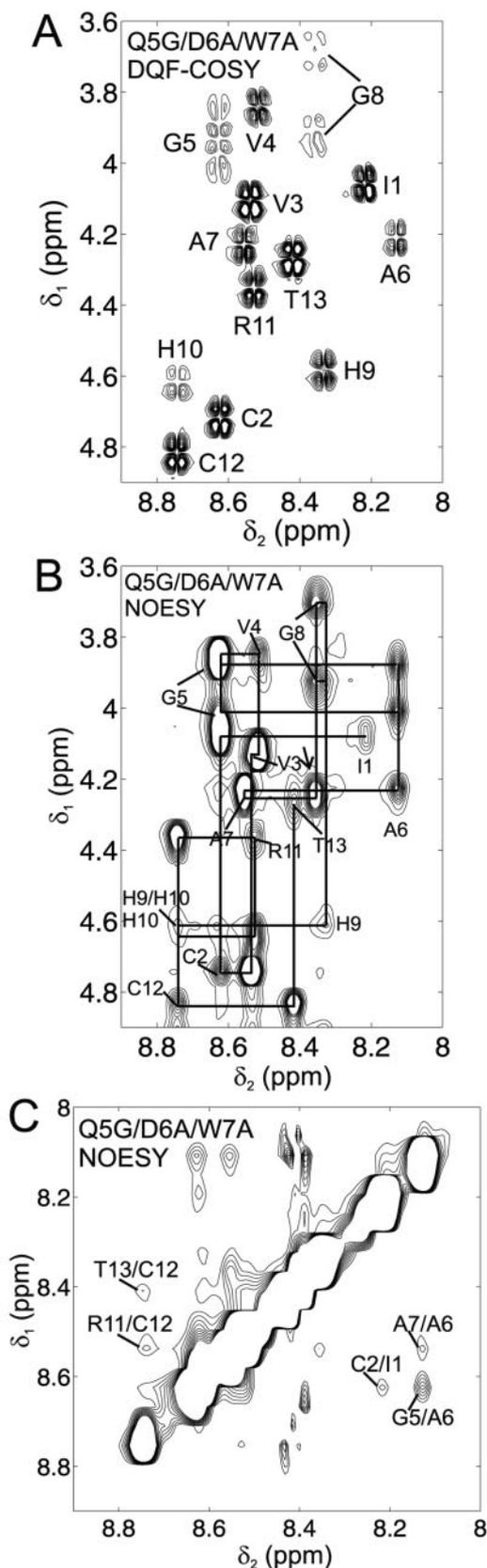
FIG. 7. **NMR spectra of the Ac-Q5G/D6A/W7A compstatin analog.** Cross-peak labeling is as in Fig. 3. *A*, portion of the $H^{\alpha}(\delta_1)$-$H^N(\delta_2)$ region of the DQF-COSY spectrum showing the backbone of the peptide. *B*, the $H^{\alpha}(\delta_1)$-$H^N(\delta_2)$ region of the NOESY spectrum. The *arrow* shows where a $H^{\alpha}(i)$-$H^N(i + 2)$ NOE should be observed if a β-turn similar to the one of the parent peptide was present. However, we cannot assign this NOE because this position is occupied by another cross-peak in the spectrum. *C*, the $H^N(\delta_1)$-$H^N(\delta_2)$ region of the NOESY

peaks are observed and marked in Fig. 6*B*. In addition, a medium/weak intensity $H^{\alpha}(i)$-$H^N(i + 2)$ cross-peak is observed corresponding to NOEs of Asp^6 H^{α}-Gly^8 H^N, which is characteristic of the presence of β-turn in the segment Gln^5-Asp^6-Trp^7-Gly^8. The segment Gln^5-Asp^6-Trp^7-Gly^8 can be further assigned as a type I β-turn because of the presence of the medium intensity $H^N(i)$-$H^N(i + 1)$ cross-peaks of Asp^6 H^N-Phe^7 H^N and Phe^7 H^N-Gly^8 H^N NOEs (Fig. 6*C*).

Based on the NOE data it appears that Trp^7 specifically is not unique for the formation of the type I β-turn, as the turn is present in the Ac-W7F analog as well. The need for participation of an aromatic residue at position 7 in the formation of the type I β-turn cannot be excluded. It is also possible that an aromatic residue at position 7 simultaneously influences the structure of the amino-terminal half of compstatin, which is part of the hydrophobic cluster. Because of loss of inhibitory activity in the Ac-W7F analog, it is possible that Trp^7 participates in binding with C3. This could be possible through a hydrogen bond involving the indole amide of Trp^7 as a donor.

The Triple Replacement $Gln^5 \rightarrow Gly/Asp^6 \rightarrow Ala/Trp^7 \rightarrow Ala$ (Ac-Q5G/D6A/W7A) Analog—In the Ac-Q5G/D6A/W7A analog Gln^5 is replaced by Gly and Asp^6 and Trp^7 are replaced by Ala. The rationale for this replacement was to introduce steric simplification and flexibility within the β-turn of the parent peptide, compstatin. This replacement resulted in an inactive analog (Table I).

Fig. 7*A* shows the $H^{\alpha}(\delta_1)$-$H^N(\delta_2)$ region of the DQF-COSY spectrum of the Ac-Q5G/D6A/W7A analog, where all residues have been identified. Chemical shift overlaps in the H^N are observed for Cys^2/Gly^5, Val^3/Arg^{11}, and His^{10}/Cys^{12} and in the H^{α} for Ala^6/Ala^7 and His^9/His^{10}. Despite the H^{α} overlaps the resulting cross-peaks are distinct (Fig. 7*A*).

Fig. 7, *B* and *C,* shows the $H^{\alpha}(\delta_1)$-$H^N(\delta_2)$ and $H^N(\delta_1)$-$H^N(\delta_2)$ regions, respectively, of the NOESY spectrum of the Ac-Q5G/D6A/W7A analog. All sequential connectivities corresponding to intra-residue $H^{\alpha}(i)$-$H^N(i)$ and short range $H^{\alpha}(i)$-$H^N(i + 1)$ NOE cross-peaks are observed and marked in Fig. 7*B*. A $H^{\alpha}(i)$-$H^N(i + 2)$ cross-peak corresponding to Ala^6 H^{α}-Gly^8 H^N NOE that if present would be consistent with the β-turn of the parent peptide, compstatin, cannot be assigned with certainty, as it would overlap with the strong intensity Ala^7 H^{α}-Gly^8 H^N cross-peak (marked with *arrow* in Fig. 7*B*). To have a type I β-turn in the same segment as the parent peptide compstatin, $H^N(i)$-$H^N(i + 1)$ cross-peaks corresponding to Ala^6 H^N-Ala^7 H^N and Ala^7 H^N-Gly^8 H^N NOEs should be present in Fig. 7*C*. From these cross-peaks only the Ala^6 H^N-Ala^7 H^N NOE is present, thus excluding structural similarity with the parent peptide compstatin. The presence of sequential Gln^5 H^N-Ala^6 H^N and Ala^6 H^N-Ala^7 H^N NOEs could be consistent with a type I β-turn in the segment Val^4-Gly^5-Ala^6-Ala^7, but because of missing of the accompanying Gly^5 $H^{\alpha}(i)$-Ala^7 $H^N(i + 2)$ NOE in Fig. 7*B*, we conclude that the Ac-Q5G/D6A/W7A analog is unstructured.

Based on the NOE data, the introduction of flexibility within the type I β-turn of compstatin resulted in both loss of the structural stability and loss of inhibitory activity. This suggests that either the type I β-turn or specific residues in the turn segment or both are necessary for C3 binding and inhibitory activity.

The Triple Replacement $Gln^5 \rightarrow Gly/Asp^6 \rightarrow Pro/Trp^7 \rightarrow Phe$ (Ac-Q5G/D6P/W7F) Analog—In the Ac-Q5G/D6P/W7F

spectrum. Cross-peaks corresponding to Gly^5 H^N-Ala^6 H^N and Ala^6 H^N-Ala^7 H^N NOEs are observed. These NOEs are consistent with the presence of type I β-turn in the region Val^4-Gly^5-Ala^6-Ala^7, which would be shifted by one residue when compared with the type I β-turn of the parent peptide compstatin. However, in the absence of the $H^{\alpha}(i)$-$H^N(i + 2)$ NOE between Gly^5 H^{α}-Ala^7 H^N (*B*) we cannot assign with certainty a β-turn.
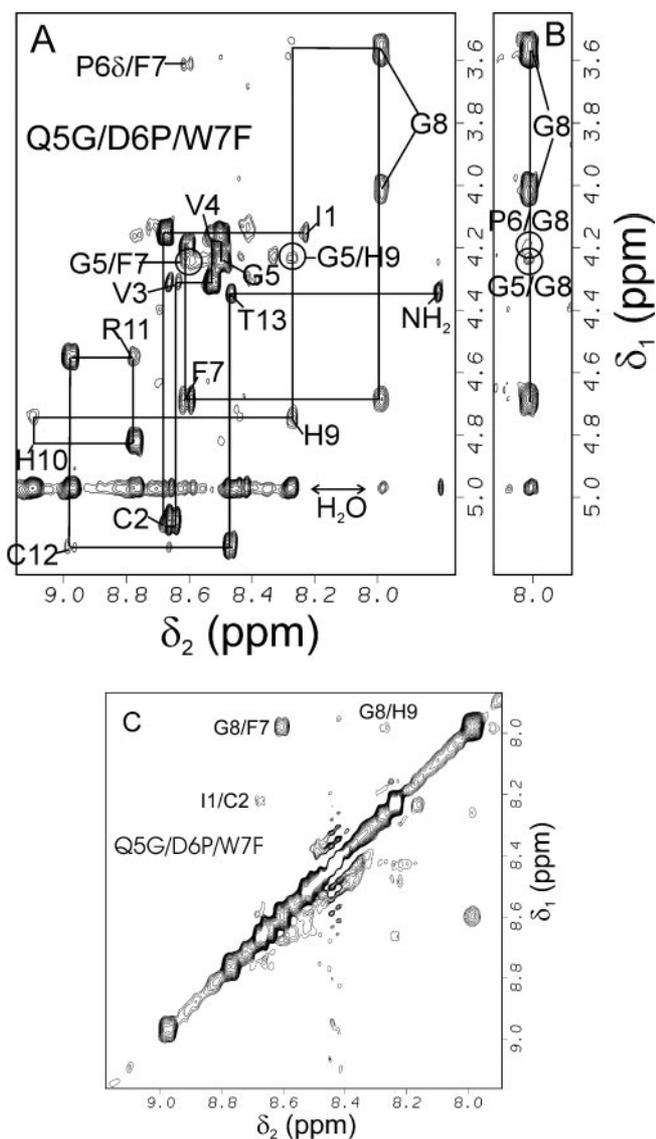
NMR Studies of Compstatin Analogs

FIG. 8. **NMR spectra of the Ac-Q5G/D6P/W7F compstatin analog.** *A,* the backbone $H^\alpha(\delta_1)$-$H^N(\delta_2)$ region of the two-dimensional NOESY spectrum. Intra-residue $H^\alpha(i)$-$H^N(i)$ and sequential $H^\alpha(i)$-$H^N(i + 1)$ NOEs are connected with *straight lines.* Additional cross-peaks characteristic of structure involving Gly[5] H^α-Phe7 H^N (*circled*), Gly[5] H^α-His[9] H^N (*circled*), and Pro[6] H^δ-Phe[7] H^N are observed. *B,* portion of *A* containing Gly[8] plotted at lower contour level, which reveals the weak Gly[5] H^α-Gly[8] H^N and the extremely weak Pro[6] H^α-Gly[8] H^N NOEs (*each circled*). *C,* the backbone $H^N(\delta_1)$-$H^N(\delta_2)$ region of the two-dimensional NOESY spectrum showing $H^N(i)$-$H^N(i + 1)$ cross-peaks.

analog Gln[5] is replaced by Gly; Asp[6] is replaced by Pro; and Trp[7] is replaced by Phe. The rationale for this replacement was to enforce the β-turn and test relation to activity. We hypothesized that this could be achieved by the following: (*a*) removal of steric hindrance imposed on the backbone from the side chain of the first residue of the type I β-turn by replacing Gln[5] with Gly; (*b*) introduction of a proline that provides a backbone bend frequently observed in type II β-turns in proteins (28); and (*c*) replacement of Trp[7] by Phe to retain, to a certain extent, bulkiness at position 3 of the turn of parent peptide, while maintaining hydrophobicity.

Fig. 8, *A* and *C,* shows the $H^\alpha(\delta_1)$-$H^N(\delta_2)$ and $H^N(\delta_1)$-$H^N(\delta_2)$ regions, respectively, of the NOESY spectrum of the Ac-Q5G-/D6P/W7F analog. Fig. 8*B* is a portion of Fig. 8*A* including NOEs involving the H^N of Gly[8], plotted at lower contour level. All sequential connectivities corresponding to intra-residue

TABLE II
Compstatin analogs with conservative replacements[a]

Peptide[b]	Sequence[c]	IC$_{50}$ (μM)[d]
Ac-V3L	Ac-I*C**L**VQDWGHH RC*T-NH$_2$	10
Ac-Q5N	Ac-I*CVV**N**DWGHH RC*T-NH$_2$	4.2
Ac-V3L/Q5N	Ac-I*C**L**V**N**DWGHH RC*T-NH$_2$	8.3
R11K	I*CVVQDWGHH **K**C*T-NH$_2$	20.2
Ac-R11S	Ac-I*CVVQDWGHH **S**C*T-NH$_2$	25
Ac-Q5N/R11A	Ac-I*CVV**N**DWGHH **A**C*T-NH$_2$	60
Ac-H9A/R11A	Ac-I*CVVQDWG**A**H **A**C*T-NH$_2$	9.9
Ac-H9A/R11dR	Ac-I*CVVQDWG**A**H**dR**C*T-NH$_2$	>1000
Ac-T13I	Ac-I*CVVQDWGHH RC***I**-NH$_2$	3.2

[a] Underlined residues/groups are points of amino acid replacement or acetylation compared to parent peptide compstatin (Table I).
[b] Ac stands for acetylated N terminus.
[c] Asterisks on the left and right of Cys[2] and Cys[12], respectively, denote disulfide-linked cysteines.
[d] Complement activities were determined by measuring alternative pathway-mediated erythrocyte lysis.

$H^\alpha(i)$-$H^N(i)$ and short range $H^\alpha(i)$-$H^N(i + 1)$ NOE cross-peaks are observed and marked in Fig. 8*A,* except for the lack of amide in Pro[6] which introduces a break. An extremely weak $H^\alpha(i)$-$H^N(i + 2)$ cross-peak between Pro[6] H^α-Gly[8] H^N is present in Fig. 8*B,* which is consistent with the presence of a very weak turn segment in Gly[5]-Pro[6]-Phe[7]-Gly[8], as was the case in the corresponding segment of compstatin. In addition, we observe a medium intensity $H^\alpha(i)$-$H^N(i + 2)$ cross-peak and weak intensity $H^\alpha(i)$-$H^N(i + 3)$ and $H^\alpha(i)$-$H^N(i + 4)$ cross-peaks corresponding to NOEs of Gly[5] H^α-Phe[7] H^N, Gly[5] H^α-Gly[8] H^N, and Gly[5] H^α-His9 H^N, respectively. These NOEs could be characteristic of a turn of an α-helix in the segment Gly[5]-Pro[6]-Phe[7]-Gly[8]-His[9], but the assignment cannot be completed using H^N-H^N NOEs because of lack of amide proton in proline. Thus, we conclude that these NOEs are consistent with the presence of undetermined structure in the segment Gly[5]-Pro[6]-Phe[7]-Gly[8]-His[9].

Based on the NOE data the radical triple replacement in the Ac-Q5G/D6P/W7F analog produced a structured segment Gly[5]-Pro[6]-Phe[7]-Gly[8]-His[9], in which a small turn populations in the segment Gly[5]-Pro[6]-Phe[7]-Gly[8] cannot be excluded. The loss of activity and possible introduction of additional structure in the Ac-Q5G/D6P/W7F analog points out the specificity of the four residues of the type I β-turn of the parent peptide compstatin for structural stability and inhibitory activity.

Activity Studies of Compstatin Analogs with Conservative Replacements—We have constructed a number of conservative replacement compstatin analogs and have tested their activity (Table II), without performing the NMR analysis, as it was deemed unnecessary. Some of these analogs are active, but only one of them has shown slightly higher activity than Ac-compstatin (Table II). When comparing the Ac-V3L, Ac-Q5N, and R11K compstatin analogs to compstatin, it appears that Val is slightly preferred than Leu at position 3; Asn is equally preferred as Gln at position 5; and Arg is more preferred than Lys at position 11 (Table II). Also, the double replacement in the Ac-V3L/Q5N analog resulted in a 2-fold lower activity than Ac-compstatin (Table II). To address the issue of proteolytic cleavage at Arg[11] during biotransformation of compstatin (13), we have prepared the Ac-R11S, Ac-Q5N/R11A, Ac-H9A/R11A compstatin analogs, none of which was more active than compstatin (Table II). It appears that Arg is a preferred amino acid at position 11, although the double replacement analog Ac-

H9A/R11A showed only about 2-fold reduced activity than compstatin because of compensation from the H9A substitution. Also, replacement of Arg[11] with dArg resulted to total loss of inhibitory activity.

To test further our hypothesis of hydrophobic clustering at the termini, we prepared the Ac-T13I analog, where Thr was replaced with the more hydrophobic Ile to enhance hydrophobicity. This analog showed slightly higher activity than compstatin (Table II), consistent with our hypothesis.

DISCUSSION

We have designed seven analogs of compstatin in which we have introduced a series of perturbations in key structural elements of their parent peptide, compstatin. The design was based on the previously determined three-dimensional structure of compstatin (14). The structure of compstatin consists of a disulfide bridge on one side and a type I β-turn on the opposite side. The disulfide bridge is part of a hydrophobic cluster, and the type I β-turn is part of a polar surface. The structural perturbations were made to test the effect of specific residue replacements in the structural stability of compstatin and their contributions in binding to C3 and complement inhibitory activity. We know that the disulfide bridge is essential for activity, and we have hypothesized that both the type I β-turn and the hydrophobic clustering at the termini are necessary for activity (1, 13, 14). Our first goal was to correlate structure with activity for each analog and for compstatin. Our second goal was to design analogs that are equally active to or more active than compstatin. Specifically, our structural perturbations were made for the following reasons: 1) to test the significance of the disulfide bridge in the formation of structure in compstatin; 2) to locally alter the structure of compstatin, outside and inside the β-turn, to test the structural stability of the β-turn; and 3) to locally alter the hydrophobic clustering to test its contribution in the formation of the β-turn. The structural analysis of the compstatin analogs was made using NMR data. We used correlation spectroscopy for proton assignments and NOE spectroscopy to elucidate NOE connectivity patterns that are consistent with structure. The known three-dimensional structure of compstatin (14) was used as a base-line structural template for our analysis. Fig. 9 summarizes the backbone NOE connectivity patterns observed for the seven compstatin analogs studied by NMR. The higher intensities of the $H^{\alpha}(i)$-$H^{N}(i + 1)$ compared with $H^{N}(i)$-$H^{N}(i + 1)$ NOEs suggest NOE averaging because of the presence of extended conformations, in addition to the observable populations of the proposed structures. This is expected because of flexibility and conformational interconversion that is present in small peptides in solution.

The C2A/C12A linear analog showed a structure consistent with the presence of a turn of a 3_{10}-helix. A 3_{10}-helix contains a type III β-turn, which is typically considered as a special case of a type I β-turn, because it differs only by 30° in ϕ_3 and ψ_3, two of four backbone dihedral angles (ϕ_2, ψ_2, ϕ_3, ψ_3) used to characterize β-turns. This suggests that the sequence of compstatin has inherent propensity to form structures consistent with a turn (helical or reverse). The C2A/C12A analog is inactive which indicates that its structure is not sufficient for inhibitory activity. It appears that the disulfide bridge of compstatin is necessary to bring together the two termini and in effect contribute in the formation of the hydrophobic clustering of residues Ile[1]-Cys[2]-Val[3]-Val[4]-Cys[12]-Thr[13].

Acetylation of compstatin effectively neutralizes the amino terminus, which in charged form (non-acetylated) disrupts the hydrophobic clustering of the termini (the carboxyl terminus is also blocked and neutral). The Ac-compstatin has shown 3-fold increase in inhibitory activity compared with compstatin (12,

FIG. 9. **Summary of backbone NOE connectivities for the seven compstatin analogs.** The *thickness* of the *bars* for $H^{N}(i)$-$H^{N}(i + 1)$ and $H^{\alpha}(i)$-$H^{N}(i + 1)$ NOEs is proportional to relative intensities, and the remaining bars simply denote connectivities. With the exception of C2A/C12A all other analogs are acetylated but are not shown in the figure for simplicity.

13). This enforces our hypothesis that the hydrophobic clustering of the termini is essential for binding to C3. The remaining six analogs studied here were acetylated.

The fourth residue of the β-turn of compstatin, Gly[8], is a favored residue at position 4 in type I β-turns in proteins because the lack of side chain of Gly provides conformation freedom for the formation of the turn. In the Ac-H9A analog we introduced more conformational freedom immediately outside the type I β-turn, following Gly[8], by replacing the bulky His[9] with the simpler Ala. The structure of this analog is consistent with the presence of a type I β-turn in the same segment as compstatin but of a slightly reduced population (or in other words a type I β-turn with slightly higher flexibility). The population of compstatin itself also suggests flexibility (14). With a similar rational we prepared the Ac-V4A/H9A/T13I analog where we introduced conformational freedom immediately outside both ends of the type I β-turn of compstatin, by simultaneously replacing brunched Val[4] and bulky His[9] with alanines. In addition, we replaced Thr[13] with the more hydrophobic Ile to enhance the hydrophobic clustering at the termini. The structure of this analog is also consistent with the presence of a type I β-turn in the same segment as compstatin but of even more reduced population than the Ac-H9A analog. Given that the Ac-H9A analog is slightly more active than Ac-compstatin, the Ac-V4A/H9A/T13I analog is as active as Ac-compstatin, and all three of them incorporate in their structures a

flexible type I β-turn, we propose that the type I β-turn is necessary for activity. Also, because the type I β-turn is flexible in all three peptides, Ac-compstatin, Ac-H9A, and Ac-V4A/H9A/T13I, it is not unlikely that flexibility is important for activity.

The third residue of compstatin, Val[3], is essential for inhibitory activity of compstatin (14). We have hypothesized that this is because of participation of Val[3] in the hydrophobic clustering of the termini, which in turn is important for binding to C3. In the Ac-V3A analog we introduced weakening in the hydrophobic clustering by replacing Val[3] with Ala. The structure of this analog is consistent with the presence of a strong type I β-turn in the same region as in compstatin. This suggests that the presence of Val[3] does not directly influence the formation of the β-turn structure, although it may influence its flexibility. The loss of inhibitory activity for the Ac-V3A analog may be attributed to the disruption of the hydrophobic clustering of the termini, which may be essential for binding to C3.

The role of Trp[7] in the formation of the type I β-turn has been intriguing to us. It has not been clear what is the significance of the hydrophobic side chain of Trp[7], which caps the β-turn and bends toward the clustering of Val[3] and Val[4] in compstatin. In the Ac-W7F analog we introduced another aromatic residue, Phe, which is more hydrophobic than Trp. The structure of this analog is consistent with the presence of a type I β-turn in the same region as in compstatin, but the analog is inactive. These results do not exclude the possibility of participation of the hydrophobic side chain in position 7 of compstatin or Ac-W7F (position 3 of the β-turn) in the formation of the turn; however, these results implicate Trp[7] but not Phe[7] in recognition and binding to C3. This is probably accomplished through the indole amide of Trp, which can act as an intermolecular hydrogen bond donor to a C3 residue.

We have proposed above, based on our results for the Ac-H9A and Ac-V4A/H9A/T13I analogs, that the type I β-turn is a necessary condition for binding to C3. Based on our results for the Ac-V3A and Ac-W7F analogs, we propose that the type I β-turn is not a sufficient condition for binding of compstatin to C3. Additional interactions of side chains may contribute to recognition and binding of compstatin to C3, and we have identified so far Trp[7] and the hydrophobic surface presented by the side chain clustering of Ile[1]-Cys[2]-Val[3]-Cys[12]-Thr[13]. We have excluded Val[4], which is also part of the hydrophobic clustering in compstatin, because even in the absence of Val[4] the Ac-V4A/H9A/T13I analog is equally active as compstatin.

In the remaining two analogs we introduced radical triple replacements inside the β-turn for turn residues 1–3, while leaving Gly at the fourth position. The analog Ac-Q5G/D6A/W7A with oversimplified turn region consisting only of glycines and alanines showed no structure. The analog Ac-Q5G/D6P/W7F, in which Pro[7] introduced a bend thought to be necessary for turn formation, was found to have undetermined structure in the region Gly[5]-Pro[6]-Phe[7]-Gly[8]-His[9]. Our results on the triple substitution analogs within the type I β-turn of compstatin together with our earlier inhibitory activity results (13, 14) suggest specificity of the residues Gln[5]-Asp[6]-Trp[7]-Gly[8] for turn formation and activity.

Finally, a number of conservative replacement analogs were tested for activity without performing parallel structural studies (Table II). From these analogs the Ac-T13I showed slightly better inhibitory activity than Ac-compstatin. From the remaining analogs we conclude that there is no preference for Gln or Asn at position 5; Val is preferred in position 3 than Leu; and Arg is preferred in position 11 than Lys. Interestingly, the Ac-H9A/R11A was found to be only about 2-fold less active than Ac-compstatin, in contrast to Ac-Q5N/R11A which was found to
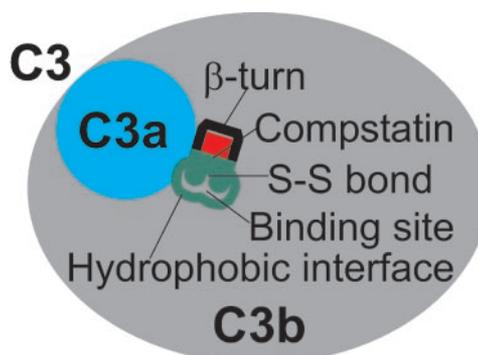

Fig. 10. **Schematic depicting the proposed binding model for C3-compstatin complex, based on binding kinetic and structural data (see text).** The polar part of compstatin, which includes the type I β-turn, is drawn in *red*, and the hydrophobic part of compstatin is drawn in *green*. The formation of the binding site is indicated by a *green line* at the site of hydrophobic interaction and by a *black line* at the site of docking of the β-turn. The binding site is on the C3b part of C3, but the smaller fragment C3a participates in the formation of the binding site.

be about 13-fold less active than Ac-compstatin. This means that some combinations of replacements can have compensatory effects in gaining or losing activity.

Overall, we conclude that the type I β-turn serves to introduce reversibility and to separate sufficiently the two sides of compstatin. At the same time the disulfide bridge at the opposite end serves to prevent the two sides from drifting apart, facilitating the formation of the hydrophobic cluster. Also, residues in the turn and in the hydrophobic patch are essential for recognition and binding to C3 and activity.

We have shown previously that compstatin binds to C3 and inhibits cleavage of C3 to C3a and C3b (the proteolytically activated form of C3) by the C3 convertase C3b,Bb (8). We have also shown that inhibition of C3 cleavage does not occur in part because of inhibition of the formation of C3b,Bb or inhibition of the formation of properdin-stabilized C3b,Bb (C3b,Bb,P; see Ref. 8). In addition, we have demonstrated that compstatin binds to C3b and C3c with 22- and 74-fold, respectively, reduced relative affinities compared with binding to native C3 (13). Binding of compstatin to C3 is biphasic following the model A + B $\leftrightarrow$ AB $\leftrightarrow$ AB*, where AB* refers to some reorganization of the binding site upon binding, although binding of compstatin to C3b and C3c is monophasic following the model A + B $\leftrightarrow$ AB (13). Based on the kinetic data we propose that the conformational change that occurs when compstatin binds to C3 involves a segment of C3a that participates in the formation of the active site to better accommodate compstatin. Fig. 10 describes a model for binding of compstatin at the interface or proximity of C3b with C3a. Based on the structural data on compstatin presented here, we propose that the recognition and binding of compstatin to C3 occurs through interactions involving the following: 1) the hydrophobic cluster of compstatin (residues Ile[1]-Cys[2]-Val[3]-Cys[12]-Thr[13]) and a partially hydrophobic pocket on C3, and 2) a knob-and-hole shape complementarity that facilitates fit of the type I β-turn of compstatin within the active pocket, with the possible aid of an intermolecular hydrogen bond between Trp[7] and a residue with a suitable acceptor on C3. Our proposed conformational change for C3a, which is responsible for the high affinity biphasic binding of compstatin to native C3, may aid binding by enhancing the hydrophobic character or the shape complementarity of the active pocket, or by facilitating the formation of a hydrogen bond with Trp[7] of compstatin, or by affecting all three.

REFERENCES

1. Sahu, A., Morikis, D. & Lambris, J. D. (2000) in *Therapeutic Interventions in the Complement System* (Lambris, J. D. & Holers, V. M., eds) pp. 75–112, Humana Press Inc., Totowa, NJ
2. Sahu, A. & Lambris, J. D. (2001) *Immunol. Rev.* **180,** 35–48
3. Lambris, J. D., Reid, K. B. & Volanakis, J. E. (1999) *Immunol. Today* **20,** 207–211
4. Walport, M. J. (2001) *N. Engl. J. Med.* **344,** 1140–1144
5. Walport, M. J. (2001) *N. Engl. J. Med.* **344,** 1058–1066
6. Lambris, J. D. & Holers, V. M. (eds) (2000) in *Therapeutic Interventions in the Complement System*, Humana Press Inc., Totowa, NJ
7. Sahu, A. & Lambris, J. D. (2000) *Immunopharmacology* **49,** 133–148
8. Sahu, A., Kay, B. K. & Lambris, J. D. (1996) *J. Immunol.* **157,** 884–891
9. Soulika, A. M., Khan, M. M., Hattori, T., Bowen, F. W., Richardson, B. A., Hack, C. E., Sahu, A., Edmunds, L. H., Jr. & Lambris, J. D. (2000) *Clin. Immunol.* **96,** 212–221
10. Nilsson, B., Larsson, R., Hong, J., Elgue, G., Ekdahl, K. N., Sahu, A. & Lambris, J. D. (1998) *Blood* **92,** 1661–1667
11. Fiane, A. E., Mollnes, T. E., Videm, V., Hovig, T., Hogasen, K., Mellbye, O. J., Spruce, L., Moore, W. T., Sahu, A. & Lambris, J. D. (1999) *Xenotransplantation* **6,** 52–65
12. Furlong, S. T., Dutta, A. S., Coath, M. M., Gormley, J. J., Hubbs, S. J., Lloyd, D., Mauger, R. C., Strimpler, A. M., Sylvester, M. A., Scott, C. W. & Edwards, P. D. (2000) *Immunopharmacology* **48,** 199–212
13. Sahu, A., Soulika, A. M., Morikis, D., Spruce, L., Moore, W. T. & Lambris, J. D. (2000) *J. Immunol.* **165,** 2491–2499
14. Morikis, D., Assa-Munt, N., Sahu, A. & Lambris, J. D. (1998) *Protein Sci.* **7,** 619–627
15. Klepeis, J. L., Floudas, C. A., Morikis, D. & Lambris, J. D. (1999) *J. Comp. Chem.* **20,** 1354–1370
16. Schreiber, S. L. (1991) *Science* **251,** 283–287
17. Dyson, H. J., Lerner, R. A. & Wright, P. E. (1988) *Annu. Rev. Biophys. Biophys. Chem.* **17,** 305–324
18. Dyson, H. J., Rance, M., Houghten, R. A., Lerner, R. A. & Wright, P. E. (1988) *J. Mol. Biol.* **201,** 161–200
19. Rose, G. D., Gierasch, L. M. & Smith, J. A. (1985) *Adv. Protein Chem.* **37,** 101–109
20. Wüthrich, K. (1986) *NMR of Proteins and Nucleic Acids*, Wiley Interscience, New York
21. Dyson, H. J. & Wright, P. E. (1991) *Annu. Rev. Biophys. Biophys. Chem.* **20,** 519–538
22. Merutka, G., Morikis, D., Bruschweiler, R. & Wright, P. E. (1993) *Biochemistry* **32,** 13089–13097
23. Dyson, H. J. & Wright, P. E. (1995) *FASEB J.* **9,** 37–42
24. Ernst, R. R., Bodenhausen, G. & Wokaun, A. (1990) *Principles of Nuclear Magnetic Resonance in One and Two Dimensions*, Oxford University Press, Oxford
25. Piotto, M., Saudek, V. & Sklenar, V. (1992) *J. Biomol. NMR* **2,** 661–665
26. Marion, D., Ikura, M. & Bax, A. (1989) *J. Magn. Reson.* **84,** 425–430
27. Richardson, J. S. (1981) *Adv. Protein Chem.* **34,** 167–339
28. Wilmot, C. M. & Thornton, J. M. (1988) *J. Mol. Biol.* **203,** 221–232
29. Koradi, R., Billeter, M. & Wuthrich, K. (1996) *J. Mol. Graphics* **14,** 51–55